REPORT DOCUMENTATION PAGE

1. REPORT DATE *(DD-MM-YYYY)*	2. REPORT TYPE	3. DATES COVERED *(From - To)*
05-05-2015	Journal Article	1 Jun 2011 – 30 Mar 2012

4. TITLE AND SUBTITLE

Terahertz Radiation: A Non-contact Tool for the Selective Stimulation of Biological Responses in Human Cells

5a. CONTRACT NUMBER
FA8650-07-D-6800-0001

5b. GRANT NUMBER
N/A

5c. PROGRAM ELEMENT NUMBER
62202F

6. AUTHOR(S)

Ibtissam Echchgadda, Jessica E. Grundt, Cesario Z. Cerna, Caleb C. Roth, Bennett L. Ibey, and Gerald J. Wilmink

5d. PROJECT NUMBER
N/A

5e. TASK NUMBER
N/A

5f. WORK UNIT NUMBER
HOEB

7. PERFORMING ORGANIZATION NAME(S) AND ADDRESS(ES)

General Dynamics Information Technology
4141 Petroleum Road
JBSA Fort Sam Houston, Texas 78234-2644

8. PERFORMING ORGANIZATION REPORT NUMBER

N/A

9. SPONSORING / MONITORING AGENCY NAME(S) AND ADDRESS(ES)

Air Force Materiel Command, Air Force Research Laboratory
711 Human Performance Wing, Human Effectiveness Directorate,
Bioeffects Division, Radio Frequency Bioeffects Branch
4141 Petroleum Road
JBSA Fort Sam Houston, Texas 78234-2644

10. SPONSOR/MONITOR'S ACRONYM(S)
711 HPW/RHDR

11. SPONSOR/MONITOR'S REPORT NUMBER(S)

AFRL-RH-FS-JA-2015-0015

12. DISTRIBUTION / AVAILABILITY STATEMENT

Distribution A: Approved for public release; distribution unlimited (P.A. Case No. TSRL-PA-2015-0096, 23 Jul 15).

13. SUPPLEMENTARY NOTES

14. ABSTRACT

Collective motions of water and of many biological macromolecules have characteristic time scales on the order of a picosecond. As a result, these biomolecules can strongly absorb terahertz (THz) radiation. Due to this absorption, THz radiation can exert a diverse range of effects on biological structures. For example, THz radiation has been shown to impact the structure, functional activity, and dynamics of macromolecules such as deoxyribonucleic acid (DNA) and proteins. THz-molecular interactions can affect several gene expression pathways and, consequently, can alter various biochemical and physiological processes in cells. Indeed, THz radiation has been shown to influence the expression of several genes within different cell types. However, a complete view of the global transcriptional responses and the intracellular canonical pathways specifically triggered by THz radiation has not been elucidated. In this study, we performed a global profiling of transcripts in human cells exposed to 2.52 THz radiation and compared the exposure responses to a thermally-matched bulk-heating (BH) protocol. Our results show that both THz radiation and BH induce a significant change in the expression of numerous messenger ribonucleic acid (mRNA) and microRNAs (miRNAs). The data also show that THz radiation triggers specific intracellular canonical pathways that are not affected in the BH-exposed cells. This study implies that THz radiation may be a useful, non-contact tool for the selective control of specific genes and cellular processes.

15. SUBJECT TERMS

Cell exposure, cellular response, global gene expression, mRNAs, miRNAs, signaling pathways, thermal effect, THz bioeffect

16. SECURITY CLASSIFICATION OF:			17. LIMITATION OF ABSTRACT	18. NUMBER OF PAGES	19a. NAME OF RESPONSIBLE PERSON
a. REPORT	**b. ABSTRACT**	**c. THIS PAGE**	SAR	20	L. Johnson
U	U	U			**19b. TELEPHONE NUMBER** *(include area code)* NA

Standard Form 298 (Rev. 8-98)
Prescribed by ANSI Std. 239.18

i

Terahertz Radiation: A Non-contact Tool for the Selective Stimulation of Biological Responses in Human Cells

Ibtissam Echchgadda, Jessica E. Grundt, Cesario Z. Cerna, Caleb C. Roth, Jason A. Payne,
Bennett L. Ibey, and Gerald J. Wilmink

Abstract—**Collective motions of water and of many biological macromolecules have characteristic time scales on the order of a picosecond. As a result, these biomolecules can strongly absorb terahertz (THz) radiation. Due to this absorption, THz radiation can exert a diverse range of effects on biological structures. For example, THz radiation has been shown to impact the structure, functional activity, and dynamics of macromolecules such as DNA and proteins. THz radiation can affect several gene expression pathways and, consequently, can alter various biochemical and physiological processes in cells. Indeed, THz radiation has been shown to influence the expression of several genes within different cell types. However, a complete view of the global transcriptional responses and the intracellular canonical pathways specifically triggered by THz radiation has not been elucidated. In this study, we performed a global profiling of transcripts in human cells exposed to 2.52 THz radiation and compared the exposure responses to a thermally-matched bulk-heating (BH) protocol. Our results show that both THz radiation and BH induce a significant change in the expression of numerous mRNAs and microRNAs. The data also show that THz radiation triggers specific intracellular canonical pathways that are not affected in the BH-exposed cells. This study implies that THz radiation may be a useful, non-contact tool for the selective control of specific genes and cellular processes.**

Index Terms—**Cell exposure, cellular response, global gene expression, miRNAs, mRNAs, signaling pathways, thermal effect, THz bioeffect.**

I. INTRODUCTION

T ERAHERTz (THz) radiation strongly interacts with biomolecular systems whose time scales are on the order of a picosecond (ps). Recent experimental and molecular dynamics simulations indicate that bulk water, interfacial water (water molecules positioned at the interface of macromolecules), and numerous macromolecules (e.g., carbohydrates, proteins, and nucleic acids) strongly absorb electromagnetic radiation with frequencies ranging from 0.1 to 10 THz, where 1 THz is equivalent to 1 ps^{-1}.

Water molecules possess potent absorption of THz radiation due to their strong dipole moment and their high intermolecular hydrogen-bond (HB) rearrangements (i.e., intermolecular stretching and bending vibrational modes) [1]–[5]. Bulk water collective HB networks have been shown to exhibit intermolecular stretching and bending vibrational modes at 5 and 1.5 THz, respectively [1], [2], [5]. Interfacial, also termed solvation, water, which plays a central role not only in stabilizing the structure of macromolecules but also in mediating their specific function [6]–[11], exhibits dynamics and vibrational motion that differ considerably from that of bulk water. Specifically, bulk water consists of four HBs that rapidly rearrange on the ps timescale, whereas interfacial water predominantly forms two HBs along the axis of a biomacromolecular solute, which makes HBs in interfacial water move slower and/or survive longer than those in bulk water [12]. Recent THz spectroscopy and molecular dynamics simulations indicate that interfacial water creates two distinct hydration shells, which extend up to 20 Å from the surface of the biomolecule [12]–[14]. These studies also indicate that the second solvation shell exhibits a prominent absorption peak between 2.4 and 2.5 THz [12] and that, over the 2.2–2.9-THz frequency range, interfacial water exhibits a higher absorption coefficient ($\mu a \approx 400 \, cm^{-1}$) than bulk water [12]. Molecular dynamics simulations confirm that these differences are a result of the difference in structure between interfacial and bulk water. In addition to the interfacial water molecules that solvate them, macromolecules also exhibit high absorption coefficients at THz frequencies largely because of their strong low frequency collective modes (i.e., skeletal and breathing modes), which occur on the ps time scale [12], [13], [15]–[22].

Due to the strong absorption of THz radiation by water and macromolecules, computational models predict that exposure to high-power THz radiation will cause an appreciable amount of energy buildup within the exposed cells. This localized energy, while too low (in the meV range) to cause ionizing damage, is predicted to result in significant local temperature rise leading to significant effects at the cellular, organelle, and macromolecular levels [23]–[28]. Recent studies investigating the biological effects of THz radiation have shown that this radi-

ation interacts with the plasma membrane [24], [25], impacting its organization, function, and permeability [24]–[28]. Several *in vitro* studies performed on biological macromolecules have shown that THz radiation can also directly affect the structure, functional activity and dynamics of DNA and proteins [26], [29]–[31].

THz radiation can also significantly change the normal process of gene expression and, consequently, can influence the cellular phenotypic properties (e.g., morphology, biochemical or physiological characteristics). In fact, a number of reports have showed that both exposure to a continuous-wave (CW) THz radiation and THz radiation from a pulsed broadband source can cause gene transcriptional alterations in skin tissues [32], [33] and various cell types [25], [34]–[39]. The recent experiments with broadband THz pulses were conducted under controlled thermal conditions and the temperature-increases were measured to be not significant. Therefore, these studies suggested that THz radiation can interact with biomolecules and cells through non-thermal mechanisms (resonance-type linear and nonlinear interactions). They also argued that the shift in gene transcriptional activity by THz radiation is in part due to a change in the molecular function of macromolecules. For example, THz irradiation may have directly caused an alteration in the breathing vibrational dynamic of DNA and proteins leading to a change in their shapes or conformational states [40]–[45], and thereby affecting chromatin organization, hindering or inducing protein-DNA binding, and/or protein-protein interactions between transcription factors and coregulators.

Several of the groups employing high-power CW THz radiation, on the other hand, believe that given the high absorption of this radiation by water in biological tissue, the THz-induced effects on gene expression can be mediated by heat (hyperthermic effects), which results from the temperature buildup during exposure [26], [28], [31]. Therefore, it is proposed that the temperature rises can cause deregulation due to unfolding, entanglement, and aggregation of intracellular and membrane proteins [46]–[53]. In this light, the question of whether cells exposed to intense CW THz radiation exhibit similar cellular effects as those exposed to a matched conventional thermal bulk-heating (BH) is important.

In this study, we aimed to identify the mRNAs, microRNAs (miRNAs), and the intracellular cascades that are specifically triggered by high-power CW THz radiation. Previously conducted experiments have demonstrated that a CW single-frequency, 2.52 THz radiation can induce a change in the expression of several genes [31], [34]–[36]. However, these studies fail to provide a comprehensive view of the global genomic and cellular responses triggered by THz irradiation. Additionally, they fail to characterize THz radiation transcriptional effect on the non-coding miRNAs. This characterization is significant given that miRNAs are considered master regulators of gene expression and are critical players in many fundamental cellular processes including development, proliferation, differentiation, death, and metabolism [54]–[58].

We conducted experiments where human Jurkat T lymphocytes were exposed to a CW, single-frequency, 2.52 THz or a thermally matched BH protocol. Global expression profiling
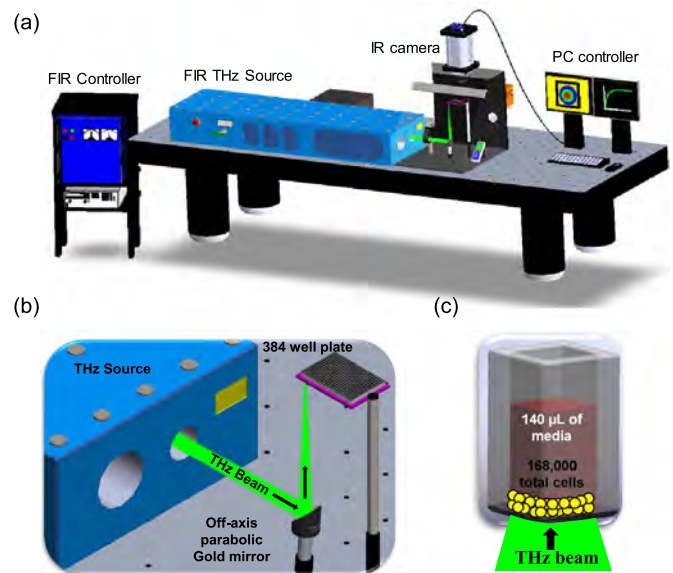

Fig. 1. Experimental setup for exposure of cells to 2.52 THz radiation. (a) Schematic representation of our custom THz exposure system. (b) Magnification of THz transmission and delivery optics. (c) Magnification of a single well with suspension cells pooled at bottom.

of transcripts and cellular responses were evaluated using microarray and bioinformatics analysis tools. Overall, our results demonstrated that THz radiation induced a significant change in the expression of specific mRNAs and miRNAs. Furthermore, the data also show that THz radiation triggered specific intracellular metabolic and signaling pathways that were not identified in the BH-exposed cells. Overall, these data provide valuable new insights that give a much clearer picture of the genes and intracellular pathways that are specifically triggered in human cells exposed to THz radiation. Additionally, the data suggest that THz radiation may be a useful, non-contact tool for the selective control of specific genes and cellular processes.

II. METHODOLOGY

A. Custom-Designed THz Exposure Enclosure

To conduct temperature-controlled THz radiation exposures, we used our custom-designed exposure system [31], [34], which consists of a temperature controller (set to 37 °C), nitrogen gas purging system, operator control area equipped with polyvinyl chloride (PVC) gloves, input ports for both short and long THz radiation cavities, optical platform, and a sapphire window for infrared (IR) thermographic measurements. Fig. 1(a)–(c) represents an illustration of our custom THz exposure setup. To ensure the chamber was exhibiting consistent heat distribution, Omega thermocouples were used to monitor the chamber's thermal stability at various spatial positions. Temperature readings were collected from the bottom to the top of the chamber using 2 cm increments (z-axis). The data showed that the exposure chamber maintained consistent optimal temperatures ($\leq$ 0.5 °C) at all positions.

B. THz Beam Manipulation and Delivery Optics

For all exposures, we used an optically pumped molecular gas THz radiation laser source (SIFIR-50 OPTL, Coherent-DEOS,
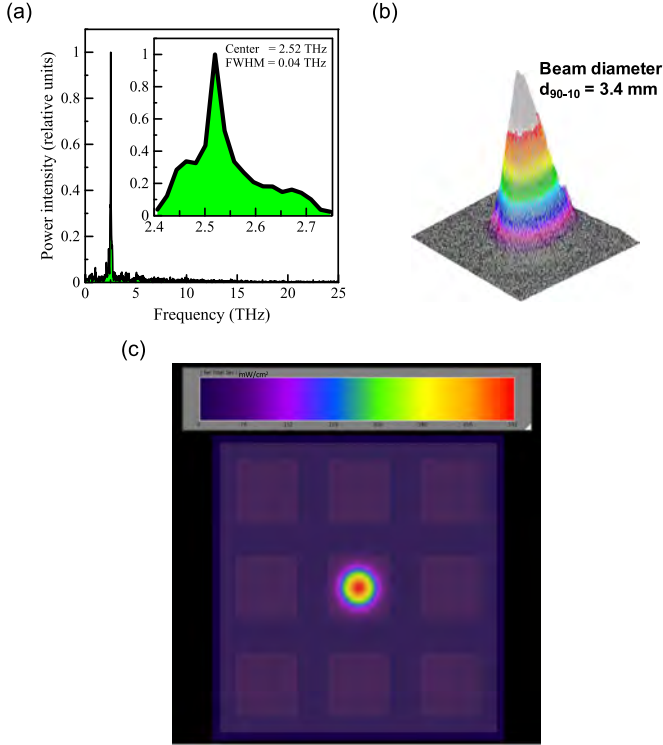
Fig. 2. (a) Plot of power intensity as function of frequency at THz. (b) Sample representative image of THz intensity beam profile. (c) FDTD model results of the THz exposure of cellular medium within the 384-well Cyclo-Olefin polymer plate geometry.

Santa Clara, CA, USA) [31], [34]. Three optical elements were used to control and deliver the THz beam from the source to the exposure plate. The first element is a microprocessor-controlled, motor-driven shutter (Sutter Instr. Co, Novato, CA). This shutter has a 25-mm diameter aperture and a 38-ms open/close time. To eliminate appreciable cutoff due to THz beam divergence, the shutter was positioned 7 cm from the opening of the short-wave cavity. Once delivered through the shutter aperture, a flat gold mirror (r = 25 mm) and a parabolic silver mirror were used to collect and focus the incident THz beam on the well plate.

C. THz Detectors and Beam Diagnostics

Prior to conducting cellular exposures, comprehensive laser beam diagnostics were performed to ensure the THz source was delivering desirable THz radiation. THz output power was measured with an Astral Vector Series H410 calorimeter (Scientech, Boulder, CO). Spatial beam profiles were evaluated using a Spiricon Pyrocam III detector array (Spiricon Inc, Logan, UT, USA). As seen in a sample image in Fig. 2(a), we found that the THz radiation source provided an irradiance of 636 mWcm^2 at a center frequency of 2.52 THz and a full-width at half-maximum (FWHM) of 0.04 THz. Using a pyroelectric array camera, we found that the intensity beam profile exhibits Gaussian distribution with a diameter of 3.4 mm, as shown in Fig. 2(b).

D. Dosimetry: Temperature History Before, During, and After THz Exposure

Jurkat cells (TIB-152, ATCC, Manassas, VA), a human T lymphocyte cell line, were maintained in Advanced RPMI 1640 media (Life Technologies, Grand Island, NY) supplemented with 10% fetal bovine serum, 10 mM Hepes, 100 units/ml penicillin, and 100 μg/ml streptomycin in a humidified, 5% CO_2 incubator at 37 °C. For all THz radiation exposure experiments, cells were plated in 384-well Cyclo-Olefin tissue culture plates (Aurora Biotechnologies, Carlsbad, CA) at a seeding density of $\sim$ 1.6 × 10^5 cells per well (140 μl total volume of cells and medium). Cells were incubated overnight and exposed the next day, as previously described [31]. The Aurora 384-well Cyclo-Olefin polymer tissue culture plates are equipped with an evaporation control system that minimizes gas exchange. In addition, for added precaution, prior to THz exposures we further sealed the top of each well plate with an optical adhesive film to prevent any suspected evaporation of media. Cells were exposed to THz radiation (ν = 2.52 THz, Φ = 636 mWcm^{-2}) from below for 40 min. The main goal for our initial set of experiments was to determine the thermal history for Jurkat cells exposed to THz radiation. To this end, we used computational and empirical dosimetric tools [31].

For the computational dosimetry, we employed finite-difference time-domain (FDTD) modeling techniques to predict the incident fields at the cells while accounting for the well plate geometry that replicate the empirical exposure conditions. Fig. 2(c) represents our modeling of the THz exposure of cellular medium within the 384-well Cyclo-Olefin polymer plate geometry. Within this simulation, the well plate geometry was modeled by cellular medium (relative permittivity = 4.4 and conductivity = 169.8 Siemens m^{-1}) surrounded by lossless polystyrene walls (relative permittivity = 2.6) mounted on top of a lossless Cyclo-Olefin polymer film (relative permittivity = 2.3). The results of this simulation indicated an incident field intensity of 532 mW/cm^2 at the location of the cell layer, corresponding to approximately 16% reduction from the 636 mW/cm^{-2} measured with the calorimeter. These simulated field values were then inputted into a finite-difference thermal solver to predict the change in temperature over time due to the THz exposure, as described before [31], [34].

For empirical temperature measurements, we used IR thermography and thermocouples. The IR camera was placed 15 cm from the media surface, and temperature measurements were acquired at 800 frames/s (SC6000, FLIR Systems Inc, Wilsonville, OR, USA). The thermocouples had the following specifications: T-type, Copper material, 0.005" diameter, Teflon insulation, and a response time of 40 ms (Omega Engineering, Inc. Stamford, CT, USA). Temperature data were collected with thermocouples before, during, and after THz exposure. For comparison, the temperature changes in sham (unexposed) control were also recorded. The sham control was placed near the THz-exposed cells in the custom-designed 37 °C preconditioned THz exposure chamber. Sample representative time-lapse IR images are provided in Fig. 3(a) and a comparative graph that depicts the thermal data for both empirical and computational methods is shown in Fig. 3(b).
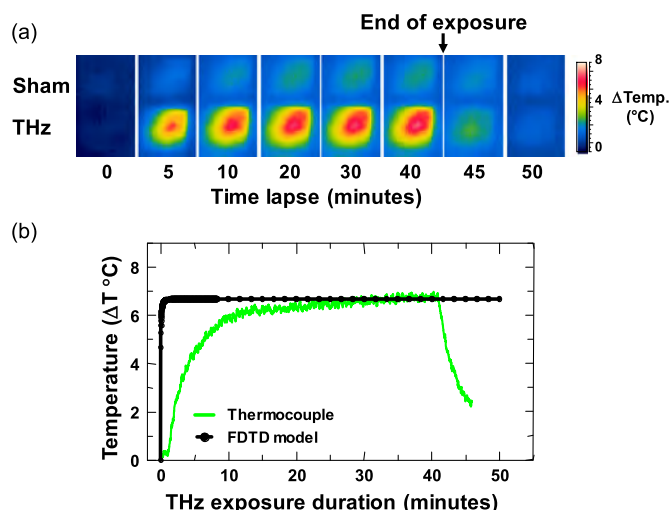
Fig. 3. Temperature history of cells exposed to 2.52-THz radiation. (a) Time-lapse IR images of temperature profiles for the surface of media in a well before, during, and after exposure. (b) Computational and quantitative temperature-time data collected for a well exposed to THz radiation using finite-difference time-domain (FDTD) modeling techniques and thermocouples, respectively.

Overall, although our computational FDTD model shows that the temperature of the well rises sharply and more quickly compared to the empirical data (thermocouples), they both flatten out at about similar level for the remainder of the exposure. Both techniques were in agreement, showing an average temperature rise of $\sim 6\,°C$ during THz-cell exposure. This change in temperature ($\Delta T\,°C$) value was used to set the thermally matched conditions of the BH. Thus, the BH-exposed cells, seeded as the THz exposed cells, in 384-well Cyclo-Olefin polymer tissue culture plates with sealed tops, were placed in a controlled water bath fixed at 44 $°C$ for 40 min. This temperature was selected to match the final temperature observed in the THz radiation exposed cells.

Additionally, we conducted MTT (3-(4,5-Dimethylthiazol-2-yl)-2,5-diphenyltetrazolium bromide) assays to determine the viability of cells exposed to THz radiation or BH. Cell viability was evaluated using MTT assays, as per manufacturer's instructions (ATCC, Manassas, VA, USA). Our experiment settings for cell exposure to THz radiation or BH resulted in a similar cellular viability measure, which was about 70% compared to sham cells.

E. RNA Isolation and Normalization

mRNAs and miRNAs were harvested from the sham, THz radiation- and BH-exposed cells using the RNeasy Mini-Kit and the miRNeasy mini kit (Qiagen, Valencia, CA, USA), respectively, as per the manufacturer's instructions. RNA extraction was performed at 4 h post-exposure. The RNAs' concentrations were assessed on a NanoDrop Spectrophotometer (NanoDrop Technologies, Wilmington, DE, USA), and the quality was measured on a 2100 Bioanalyzer (Agilent Technologies, Santa Clara, CA). RNA samples with a RNA Integrity Number greater than 9.5 were subjected to mRNA and miRNA microarray analysis.

F. mRNA Microarrays and PCR

To determine the effect of THz radiation and BH exposures on mRNA expression, we conducted microarray analysis for each exposure condition (sham, THz radiation, and BH) in triplicate using the Affymetrix GeneChip Human Genome U133 (HG-U133 plus 2.0 Array that contains 54 675 probe sets, Asuragen Services, Austin, TX, USA). Briefly, two micrograms of RNA were used for preparation of biotin-labeled targets (cRNA) using MessageAmp-based protocols (Ambion, Inc.). Labeled cRNA was fragmented and used for array hybridization and washing. The cRNA was mixed with a hybridization cocktail, heated to 99 $°C$ for 5 min, and then incubated at 45 $°C$ for 5 min. Hybridization arrays were conducted for 16 h in an Affymetrix Model 640 hybridization oven (45 $°C$, 60 rpm). Arrays were washed and stained on a FS450 Fluidics station and scanned on a GeneChip Scanner 3000 7G. Image signal data, detection calls, and annotations were generated for every gene using the Affymetrix Statistical Algorithm MAS 5.0 (GeneChip Operating Software v1.3). A $\log_2$ transformation was conducted and a Student's t-test was performed for comparison of the two groups (sham and exposed). Multiple testing corrections using Benjamini and Hochberg methods were used to determine the false discovery rate, and genes with statistically significant results were identified using Bonferroni correction procedures ($-\log 10\ p_{\text{cutoff}} > 6.04$) [59]. For interpretation of the results, the Ingenuity Pathways Analysis tool (IPA, version 8.7, Ingenuity Systems Inc., Redwood City, CA, USA[1]) was used. IPA is a web-based software application that enables filtering and dataset comparisons to identify biological mechanisms pathways and functions most relevant to experimental datasets or differentially expressed genes. The cutoff criteria for IPA analysis were an absolute value of $\log_2$ ratio ≥ 2 and a $p - \text{value} \leq 0.05$. Other web-based resources were used to complement the interpretation of the data. These included the GeneCards Human Gene Database (http://www.genecards.org/) and The HUGO Gene Nomenclature Committee (HGNC, http://www.genenames.org/). A few selected target mRNAs identified in the microarray analysis were validated using quantitative real-time polymerase chain reactions (qRT-PCR). Runs were performed on a StepOnePlus system using TaqMan RNA-to-CT 1-Step Kits and TaqMan Assays (Applied Biosystems by Life Technologies). Calibrator RNA was used as a control. PCR was conducted using a three-program LightCycler protocol.

G. miRNAs Microarray Analysis and PCR

For the miRNA microarrays, an Affymetrix GeneChip (DiscovArrayTM, Asuragen Services) was used, which included probes of all miRNAs from the Sanger miRBase and more than 12,000 predicted miRNAs [60]–[66]. For each probe, a two-sample t-test for empirical Bayes variance estimates was used. Probes with $p - \text{values} \leq 0.05$ were determined to be statistically significant. Normalized $\log_2$ transformed intensity values were analyzed using JMP Genomics 3.2 (SAS Institute, Cary, NC). IPA was used for further refinement and interpretation of miRNA microarray data. The analysis cutoffs were set
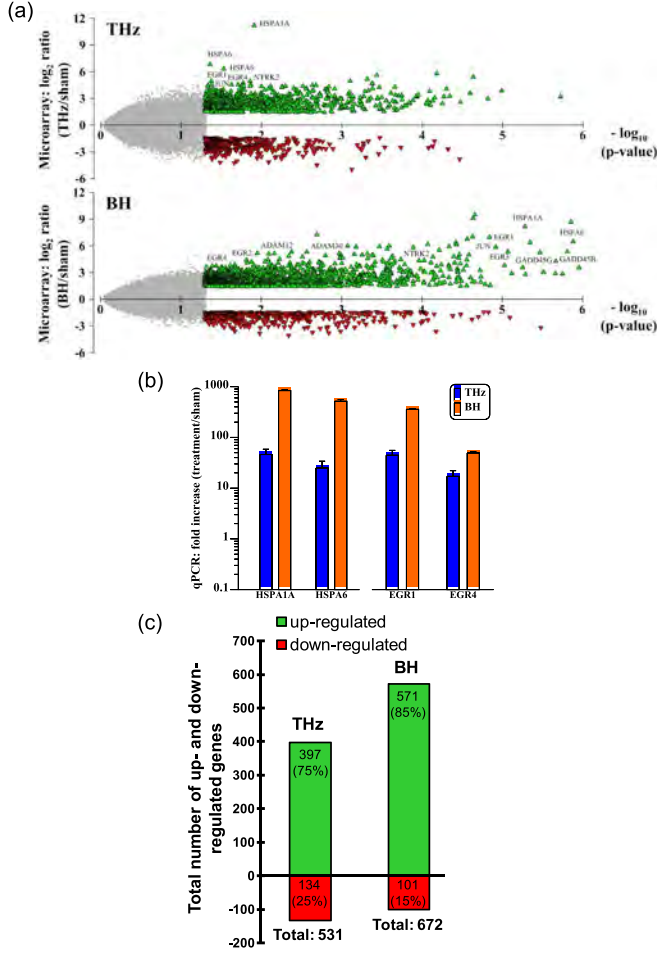
Fig. 4.   Differential expression profiles of several mRNAs in THz and BH exposed cells. (a) Volcano plots of the gene expression profiles, where the magnitude of differential expression ($\log_2$ fold-change) is plotted versus the level of statistical significance ($-\log_{10}$ p-value). Up-regulated and down-regulated genes with absolute $\log_2$ ratios ≥ 2 and $p-$values ≤ 0.05 are depicted with green and red triangle symbols, respectively. Genes denoted with light gray symbols were not significantly different. (b) qRT-PCR validation of the change in expression of selected mRNAs. (c) Total number of up- and down-regulated genes for THz and BH exposures. Using IPA, the data show that 531 and 672 genes were differentially expressed in THz and BH, respectively.
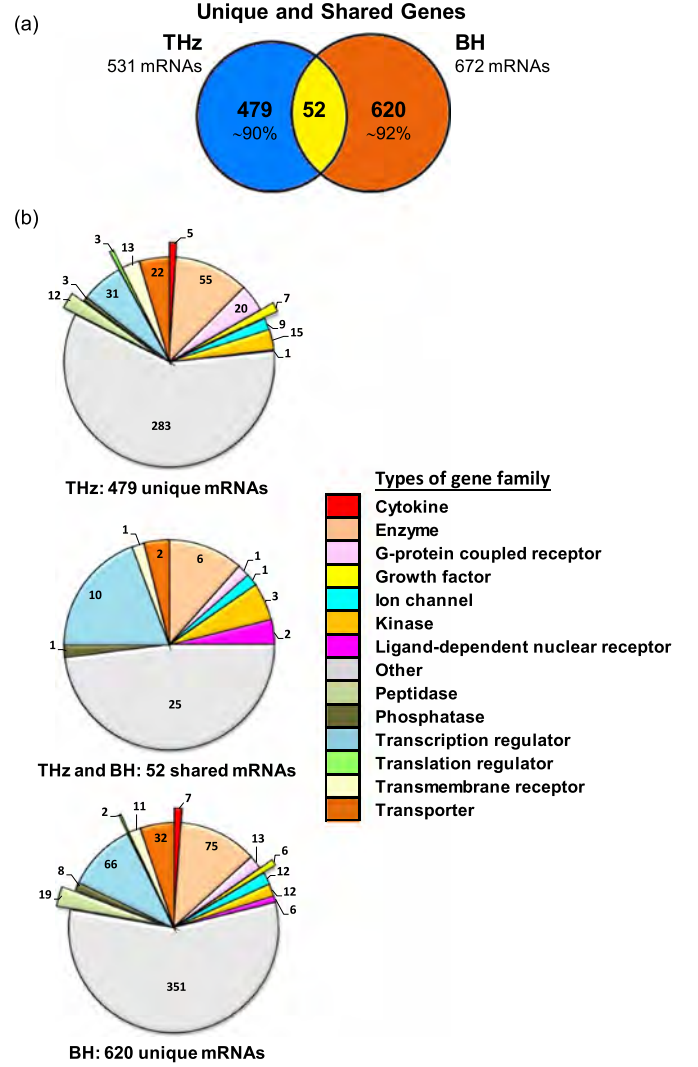

Fig. 5.   Identification of unique and shared mRNAs. (a) Venn diagram indicating the number of unique and common differentially expressed mRNAs in each exposed group. (b). Gene family of the unique and shared genes. The pie chart sectors represent the number of genes associated with each family as indicated in the legend. The protruded sectors represent the four gene families (cytokine, growth factor, peptidase, and translation regulator) that did not display shared genes between THz and BH exposures.

at $p-$values ≤ 0.05 and an absolute value of $\log_2$ ratio ≥ 0.59 (equivalent to 1.5 fold change in expression).

III. RESULTS

A. Global mRNAs Expression Profiles for Cells Exposed to THz Radiation or BH

To get a comprehensive view of the transcriptional response to THz radiation, Jurkat cells were exposed to 2.25 THz radiation or BH and microarray gene chips were used to quantify the expression levels of mRNAs in each exposure condition versus control sham (unexposed cells). Since the microarrays provide data for nearly 60,000 mRNA targets, volcano plots were created to best visualize the global distribution of the mRNAs expression profiles for THz radiation and BH, as presented in Fig. 4(a). In these plots, the level of statistical significance (p-value) for each mRNA is plotted against the fold change of expression magnitude relative to sham. mRNAs with the highest level of statistical significance appear on the

right side of the plot. Significantly up-regulated mRNAs appear towards the top of the plot (denoted with green triangles), whereas significantly down-regulated mRNAs appear towards the bottom (denoted with red triangles). The gray color represents the mRNAs that were considered unchanged. Overall, the global changes in mRNA expression profiles were similar for each exposure condition since 1162 and 1200 mRNA probes were differentially expressed in the THz radiation and BH exposure conditions, respectively. Fig. 4(b) shows a validation of the changes in mRNAs expression of few mRNAs probes in the array using qRT-PCR. These data show that the mRNAs expression levels were in agreement with those obtained in the microarray study.

IPA software was used to refine the microarray data. Using a $p-$value ≤ 0.05 and an absolute $\log_2$ ratio ≥ 2 (equivalent to four-fold change) cutoffs, 531 and 672 distinct mRNAs were identified as differentially expressed in THz radiation and BH
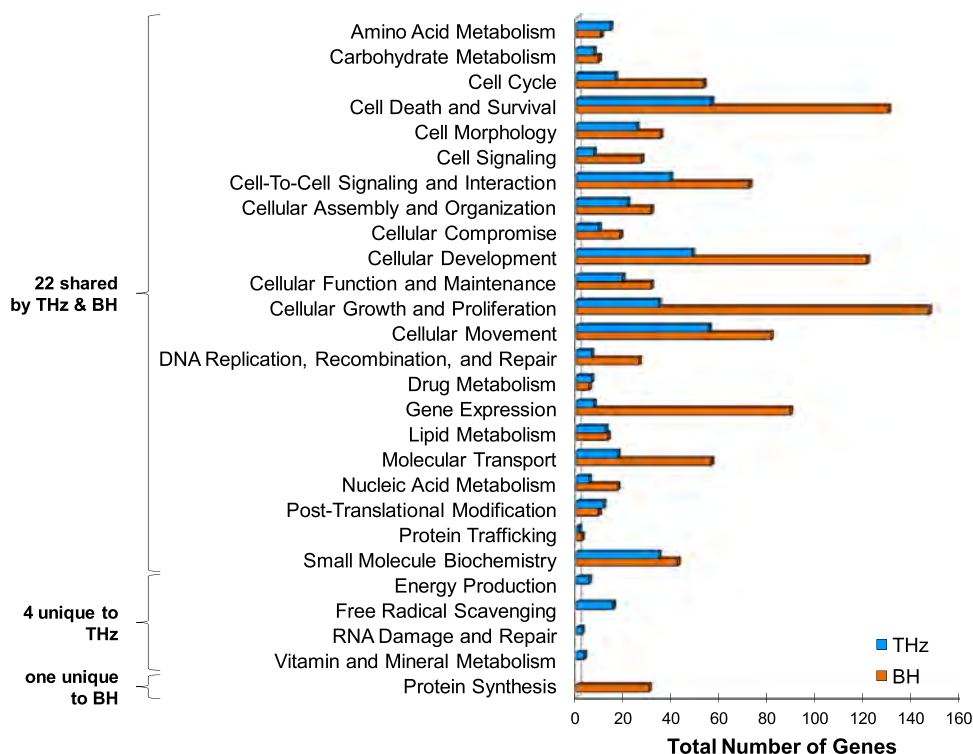
Fig. 6. Cellular and molecular functions associated with the mRNAs expressed in cells exposed to THz radiation and BH. The graph represents the molecular and cellular functions relative to the total number of mRNAs associated with each function. Twenty-two biological functions are common to THz and BH, four are unique to THz and one function is unique to BH.

exposure, respectively, as shown in Fig. 4(c). In both THz radiation and BH-exposed cells, the number of up-regulated mRNAs was higher than that of down-regulated mRNAs. The up-regulated mRNAs were 75% and 85% at four hours post THz radiation and BH exposure, respectively.

To determine whether any of the differentially expressed mRNAs were scored in both or solely in THz radiation or BH exposed cells, a biomarker comparison analysis was performed using IPA. This tool allowed us to separate the identified mRNAs into three groups: unique to THz radiation, unique to BH, and shared between THz radiation and BH. As shown in the Venn diagram in Fig. 5(a), there were a total of 479 and 620 mRNAs that were unique to THz radiation and BH exposure, respectively. Additionally, there were 52 mRNAs shared by both THz radiation and BH exposures. The 52 common mRNAs represent less than 10% of the combined total differentially expressed mRNAs after exposure to THz radiation or BH. Thus, this considerable difference in differentially expressed mRNAs between THz and BH exposures suggests that the intracellular pathways triggered in either THz radiation or BH might be vastly different.

The altered mRNAs in each group were further separated by their corresponding gene families. The pie charts in Fig. 5(b) illustrate the gene families related to the unique and shared genes as well as the number of genes for each family. The gene families are color coded as depicted in the legend. The differentially expressed genes belong to thirteen known families (cytokines, enzymes, G-protein coupled receptors, growth factors, ion channels, kinases, ligand-dependent nuclear receptors, peptidases, phosphatases, transcription regulators, translation regu-

lators, transmembrane receptors, and transporters) in addition to genes that were grouped by IPA in "other" gene families. There were a few shared genes in most gene families except for cytokines, peptidases, growth factors, and translation regulators families, as represented by the protruded sectors in Fig. 5(b). In these four gene families, the differentially expressed genes identified were all unique to either THz radiation or BH gene group.

B. Biological Functions of the THz and BH Differentially Expressed mRNAs

After identification of the mRNAs that were differentially expressed in response to THz radiation and/or BH, a characterization of each gene's primary cellular and molecular functions was also performed. The bar graph in Fig. 6 represents the total number of genes associated with each biological function. The differentially expressed genes in THz radiation and BH shared 22 cellular and molecular functions. Four biological functions (energy production, free radial scavenging, RNA damage and repair, and vitamin and mineral metabolism) were unique to genes from the THz radiation exposure, and one function (protein synthesis) was unique to genes from the BH exposure.

C. Pathway Analysis of Microarray mRNAs Data

IPA was also used to determine the canonical pathways that were affected in cells in response to THz radiation and BH. 54 metabolic pathways and 211 signaling pathways were scored in THz radiation exposure, whereas 45 metabolic pathways and 155 signaling pathways were scored in BH exposure. After setting the significant likelihood cutoff of all canonical pathways at
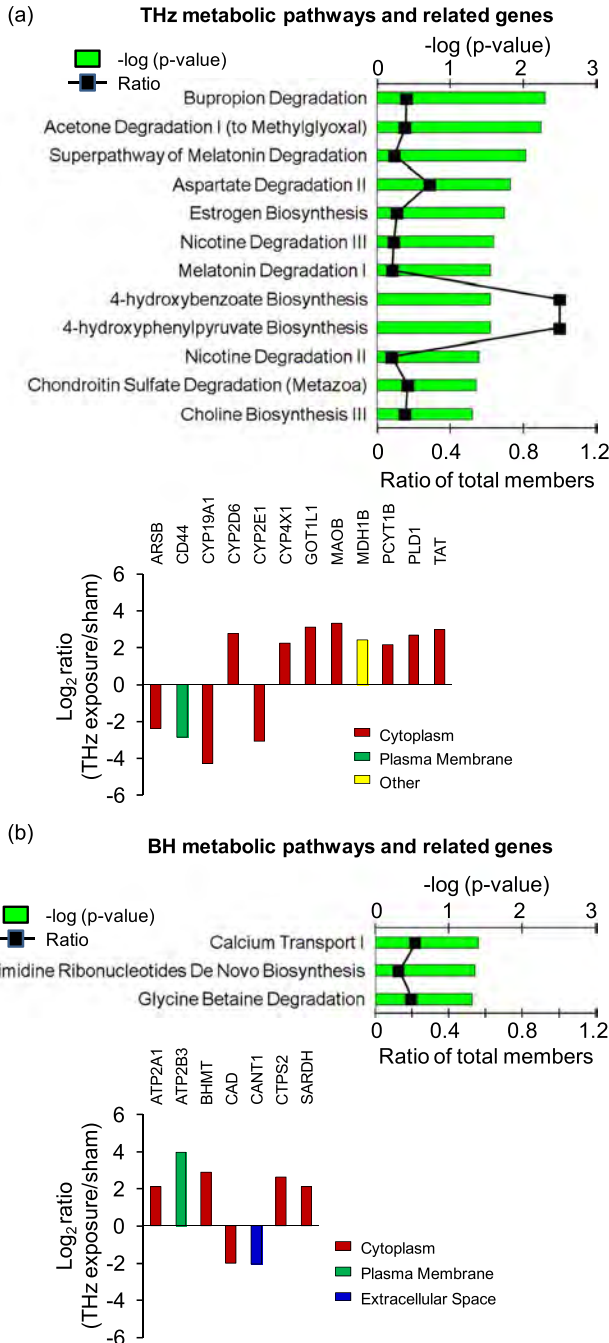
Fig. 7. THz radiation and BH induce distinct sets of metabolic pathways. (a) Significant metabolic pathways and related differentially expressed genes from THz radiation exposure. (b) Significant metabolic pathways and related differentially expressed genes from BH exposure. The metabolic pathways significance cutoff was set at threshold value (p − value ≤ 0.05). The -log (p-value) is the maximum p-value for all of the genes in each particular canonical pathway family. The ratio plot indicates the number of the genes expressed at each time point relative to the total number of genes in that particular metabolic pathway group. Bar graphs that represent the magnitude of the $\log_2$ fold-change in expression of the genes associated with the scored metabolic pathways in THz radiation or BH exposure compared to sham are shown in (a) and (b) lower panels.

the threshold value (p − value ≤ 0.05), 12 metabolic pathways and 18 signaling pathways were scored significant in the THz exposure, as seen in Fig. 7(a) and Fig. 8(a), respectively. For

the BH exposure, three metabolic pathways and 13 signaling pathways were significant, as shown in Fig. 7(b) and Fig. 9(a), respectively. All the significantly affected canonical pathways in THz radiation and BH exposures were unique to either exposure. In fact, no overlap in the metabolic or signaling pathways between THz radiation and BH exposures was observed.

Next, the significant canonical pathways were sorted by their respective categories in order to get a clear picture of their roles. The metabolic pathways associated with THz exposure are involved in processes of degradation, utilization, and detoxification, whereas BH metabolic pathways are linked to biosynthesis and transport. For the THz radiation and BH significantly scored signaling pathways, although the signaling pathways were specific to the type of exposure, most belong to four pathway categories that are present in both THz radiation and BH. These pathway categories are cellular growth proliferation and development, intracellular and second messenger, organismal growth and development, cellular immune response, and nervous system, as shown in Figs. 8(a) and 9(a), top panels. The signaling pathway categories that were exclusive to either THz radiation or BH exposure included growth factor, cell cycle regulation and disease-specific signaling pathways in THz radiation exposure, and cardiovascular, cytokine, and nuclear receptor signaling pathways in BH exposure.

The THz radiation and BH differentially expressed genes that are associated with the significantly scored pathways were then determined. Twelve and seven differentially expressed genes were identified for the metabolic pathways of THz radiation and BH, respectively. Bar graphs of the effects of THz radiation or BH on the expression profile of the transcripts from these genes are shown in the lower panels of Fig. 7(a) and (b). These bar graphs represent the $\log_2$ fold-change in expression in THz radiation or BH exposure compared to sham. On the other hand, 46 and 73 differentially expressed transcripts were identified for THz radiation and BH signaling pathways, respectively. Figs. 8(b) and 9(b) show bar graphs representing the effect of THz radiation or BH on the expression profile of these mRNAs compared to sham. Notably, the THz radiation and BH altered genes did not display a cellular component specific expression but, rather, they included genes that are expressed from all cellular locations, namely, cytoplasm, nucleus, plasma membrane, extracellular space and others (i.e., signalosome, mitochondrial matrix or unknown), as shown in Figs. 8(b) and 9(b).

Furthermore, using IPA and available web-based resources, the biological process associated with the signaling pathways related genes were characterized. Some of these genes are involved in precise biological processes; however, many are linked to multiple key biological processes, as seen in Figs. 8(b) and 9(b). Therefore, for uniformity, these genes were classified based on top key biological processes and overlaps. The results show that THz radiation and BH exposures shared biological processes linked to transcription regulation, transport, and cell signaling and signal transduction. Nonetheless, the genes associated with these processes were entirely different between THz radiation and BH, except for two genes (marked with asterisks): the transcription factor JUN (Jun Proto-Oncogene) that was induced 10-fold by THz radiation and 74-fold
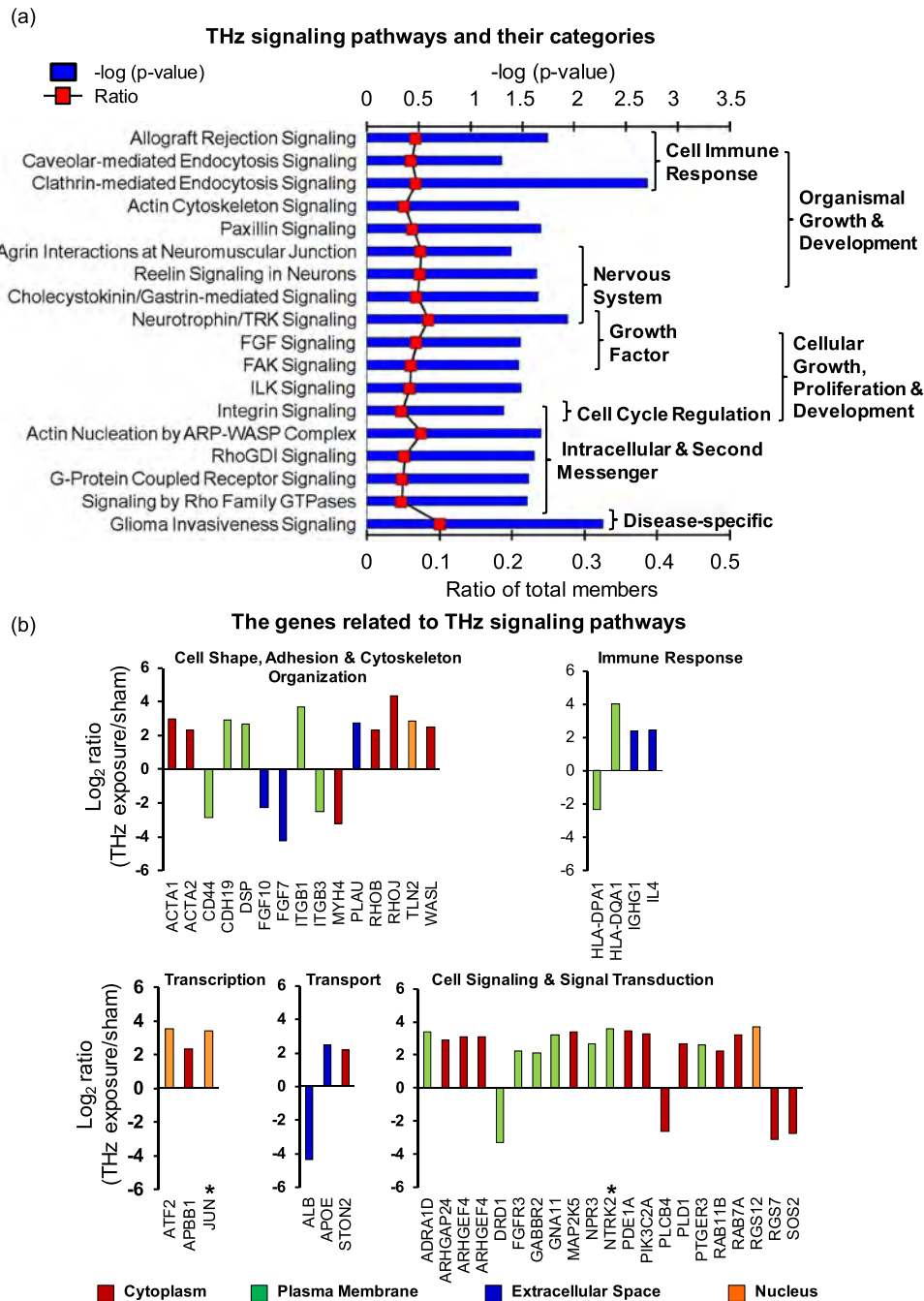
(a)

(b)

Fig. 8. THz radiation signaling pathways and related genes. (a) Significant signaling pathways scored in THz radiation exposure. The signaling pathways significant likelihood cutoff was set at threshold value (p − value ≤ 0.05). The − log (p-value) is the maximum p-value for all of the genes in each particular canonical pathway family. The ratio plot indicates the number of the genes expressed at each time point relative to the total number of genes in that particular signaling pathway group. (b) The differentially expressed genes associated with the THz significant signaling pathways. Bar graphs represent the magnitude of the $\log_2$ fold-change in expression of the genes compared to sham. The THz radiation differentially expressed genes were grouped according to their top or overlapping biological processes as shown.

by BH and the kinase NTRK2 (neurotrophic tyrosine kinase receptor type 2) that was induced 12-fold by THz irradiation and 8-fold by BH.

The results also show that the major difference between experimental groups was that THz radiation exposure specifically altered genes involved in biological processes of immune response, cell shape and adhesion, and cytoskeleton organization. Examples of the genes [shown in Figs. 4(a) and Fig. 8(b)] included the immune response genes [i.e., IL4 (interleukin 4) and

IGHG1 (immunoglobulin heavy constant gamma 1)], the actin genes ACTA1 (alpha-actin-1) and ACTA2 (alpha-actin-2), and the cell adhesion genes ITGB1 (integrin Beta-1), ITGB3 (integrin Beta-3), CDH19 (cadherin-19), MYH4 (myosin-4), RHOB (ras homolog family member B) and TLN2 (talin 2), and the actin cytoskeleton organization molecules such as RHOJ (ras homolog family member J), FGF (fibroblast growth factor) 7, FGF10, and WASL (Wiskott-Aldrich syndrome-like)). Alteration in the expression of such genes underscores the signif-
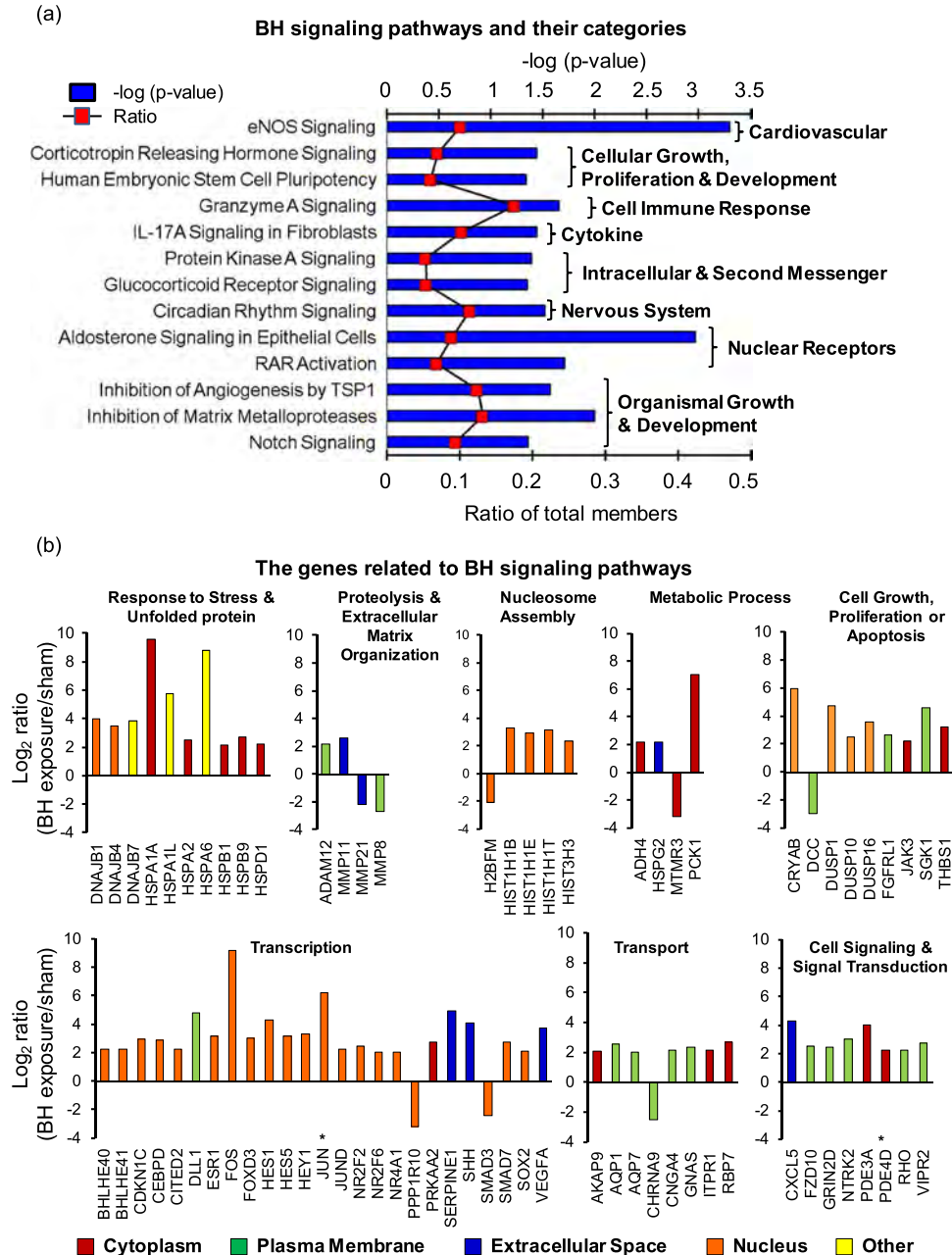
Fig. 9. BH signaling pathways and related genes. (a) Significant signaling pathways scored in BH exposure. The signaling pathways significant likelihood cutoff was set at threshold value (p − value ≤ 0.05). The − log (p-value) is the maximum p-value for all of the genes in each particular canonical pathway family. The ratio plot indicates the number of the genes expressed at each time point relative to the total number of genes in that particular signaling pathway group. (b) The differentially expressed genes associated the BH significant signaling pathways. Bar graphs represent the magnitude of the $\log_2$ fold-change in expression of the genes compared to sham. The BH differentially expressed genes were grouped according to their top or overlapping biological processes as shown.

icance of signaling pathways such as the Actin Cytoskeleton Signaling and the Actin Nucleation by ARP-WASP complex signaling in response to the THz radiation exposure.

BH exposure [shown in Figs. 4(a) and 9(b)] specifically affected the expression of genes implicated in: 1) response to heat and unfolded protein, which included the heat shock protein (HSP) 70 genes (e.g., HSPA1A, HSPA6, HSPA1L and HSPA2), HSP40 genes (e.g., DNAJB 1, 4 and 7), as well as smaller HSPs like HSP27 gene (HSPB1) and HSP60 gene (HSPD1); 2) proteolysis and extracellular matrix organization genes such as genes from the Matrix Metallopeptidase (MMP) family (e.g., MMP8, MMP11, MMP21) and from the A Disintegrin and Metallopro-

tease family (e.g., ADAM 12 and 30); 3) cell growth, proliferation or apoptosis (e.g., DUSP (dual specificity phosphatase) 1, 10 and 16, JAK (Janus kinase) 3, SGK (serum/glucocorticoid regulated kinase) 1, GADD (growth arrest and DNA-damage-inducible) 45B and 45G); 4) transcription regulatory molecules and immediate early genes, which included JUN, JUND (jun D proto-oncogene), FOS (FBJ murine osteosarcoma viral oncogene homolog), FOSB, EGR (early growth response) 1, 2, 3 and 4; and 5) nucleosome assembly (e.g., HIST (histone cluster) 1H1 and 3H3) and a few more linked to metabolism of alcohol, carbohydrate or lipid, or small molecules. As seen in Fig. 4(a), of all the BH signaling pathways related genes, only HSPA1A,
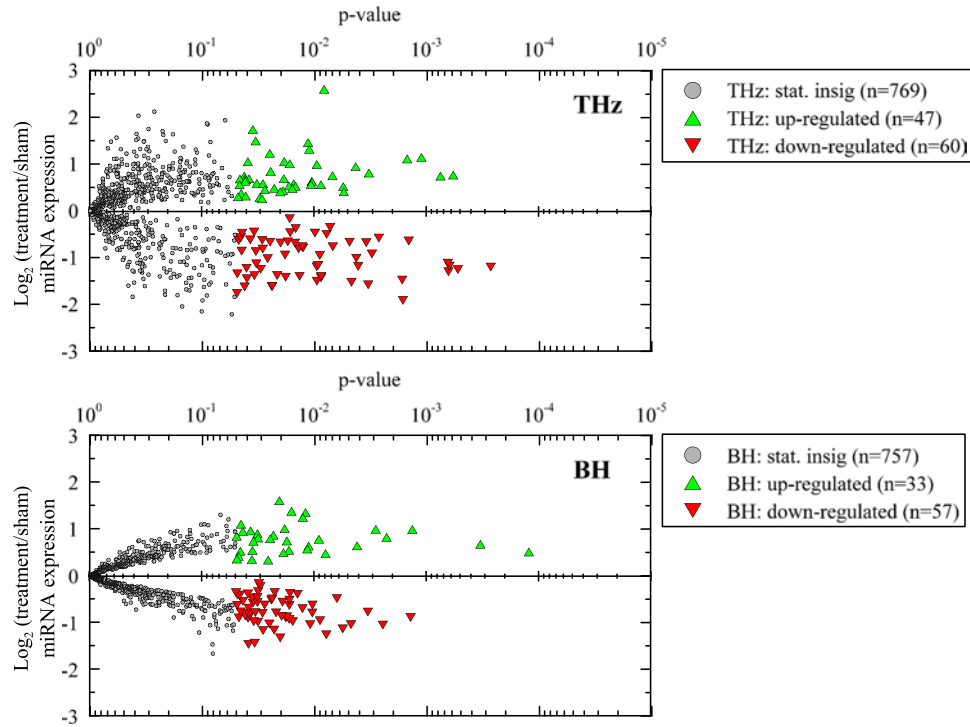
Fig. 10. THz radiation and BH alter the expression of several miRNAs. Volcano plots of the global expression profile of miRNAs. The signal difference ($\log_2$) ratio is plotted versus the level of statistical significance (p-value) of all miRNA in the microarray for THz (upper panel) and BH (lower panel) in exposed cells compared to sham. Up-regulated and down-regulated miRNAs with $p-$values ≤ 0.05 are depicted with green and red triangle symbols, respectively. Insignificant genes are denoted with light gray circle symbols. A total of 107 (47 up-regulated and 60 down-regulated) and 90 miRNAs (33 up-regulated and 57 down-regulated) have significant p-values for THz radiation and BH exposure, respectively.

HSPA6, EGR1, EGR4, JUN and NTRK2 were also significantly altered by THz exposure.

D. THz Radiation and BH Induce Differential Expression of Several miRNAs

We previously demonstrated that dermal fibroblasts differentially express a specific group of miRNAs when exposed to hyperthermic stress [66]. Since 2.52 THz induces a temperature increase in exposed Jurkat cells, we sought to determine whether THz radiation exposure would impact the expression of miRNAs similarly to thermally-matched BH exposure. miRNA microarrays were performed to identify differentially expressed miRNAs in cells four hours post-exposure. A global view of the miRNA profiles is provided as a volcano plot in Fig. 10. In these plots, $\log_2$ signal difference ratio relative to the p-value of all miRNAs in the microarray was mapped for THz (upper panel) and BH (lower panel) exposures compared to sham. Up-regulated miRNAs appear towards the top of the plot (denoted with green triangles), whereas down-regulated miRNAs appear towards the bottom of the graph (denoted with red triangles). The significance value was set at a $p-$value ≤ 0.05. Thus, the gray color circles represent the miRNAs that were statistically unchanged. In THz radiation-exposed cells, the expression of 107 miRNAs was significantly changed, of which 47 were up-regulated and 60 were down-regulated. Comparatively, in BH-exposed cells, 90 miRNAs displayed a significant change in their expression pattern, with 33 up-regulated and 57 down-regulated.

An additional significance cutoff was set for the $\log_2$ signal difference ratio, followed by IPA to perform miRNA biomarker comparison analysis. With this extra criterion, the expression of 66 and 53 miRNAs was significantly altered (fold change $\geq$ 1.5) by THz radiation and BH exposure, respectively. As presented in the Venn diagram [Fig. 11(a)], of these miRNAs, 57 were unique to THz radiation exposure, 44 were unique to BH exposure, and nine were common to both exposures. These numbers indicate that less than 17% of the differentially expressed miRNAs in THz radiation and BH were shared. Fold changes in expression of these shared and unique miRNAs compared with sham are shown in Fig. 11(b)–(d). Five of the shared miRNAs were down-regulated in both THz radiation and BH exposed cells, whereas four miRNAs (miR-576-5p, miR-526a, miR-362-5p, and miR-208a-3p) displayed a differential change in expression pattern between THz radiation and BH exposures. These miRNAs (marked with asterisks) were down-regulated by THz radiation while induced by BH.

Next, to determine target mRNAs for the altered miRNAs, IPA was used to create a miRNA-mRNA pairing analysis for the significantly differentially expressed miRNAs and mRNAs in THz radiation or BH exposure. From the THz-irradiation miRNA-mRNA pairing, 48 of the 66 altered miRNAs have 345 putative (predicted or experimentally observed) target mRNAs. In the BH exposure miRNA-mRNA pairing, there were 42 of the 53 altered miRNAs that have 438 putative target mRNAs. As expected, a number of these miRNAs have multiple sets of target mRNAs. As an example, Table I presents the result
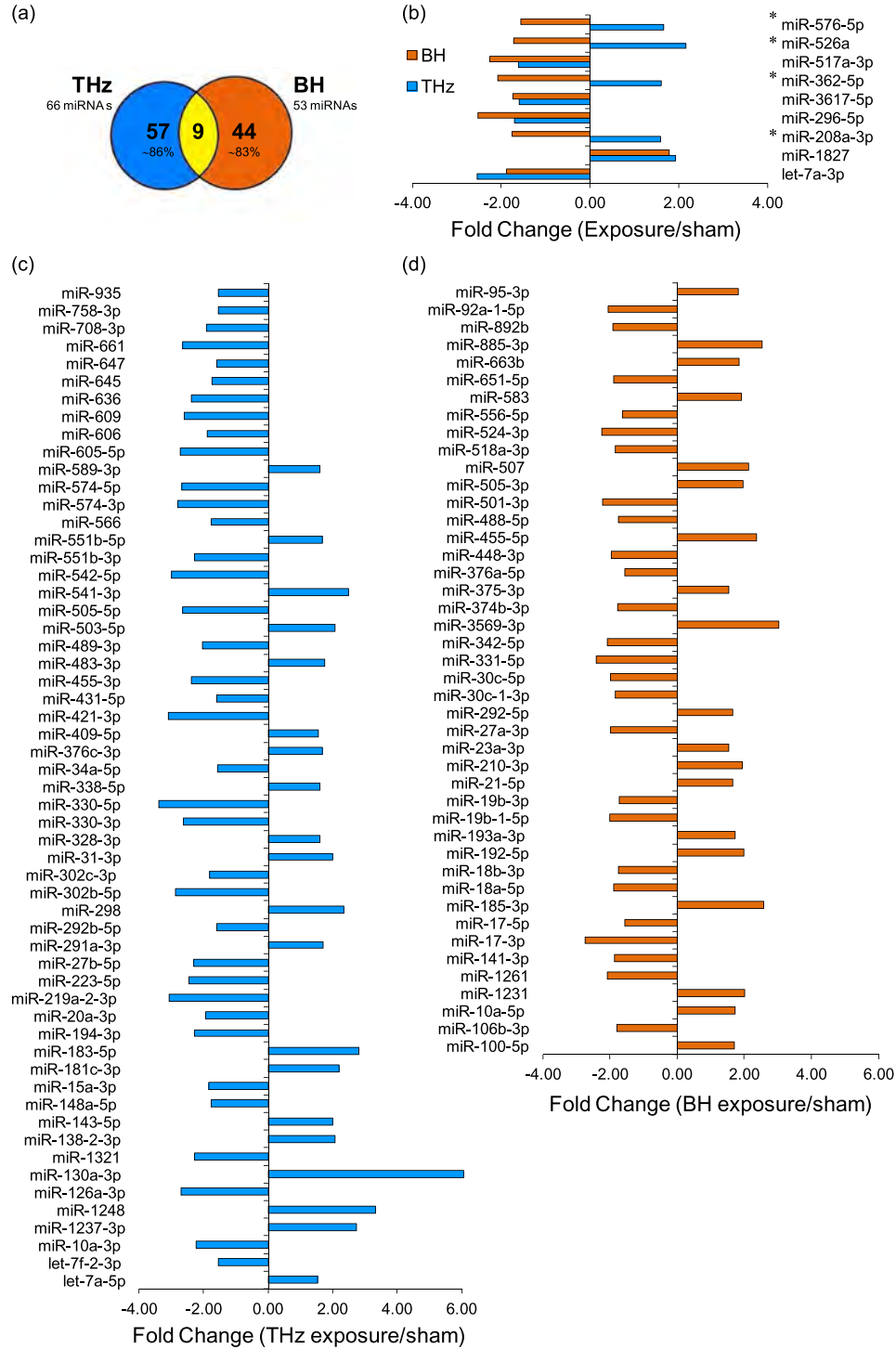
Fig. 11. Unique and shared miRNAs. (a) Venn diagram indicating the number of unique and shared miRNAs exhibiting a significant level of differential expression in THz radiation and BH exposures. The significant cutoffs were set as fold change value ≥ 1.5 and a p $-$ value ≤ 0.05. (b) Bar graph representing the fold change in expression of the shared miRNAs in THz radiation and BH exposure compared to sham. (c) Bar graph representing the fold-change in expression of the unique miRNAs in THz radiation compared to sham. (d) Bar graph representing the fold-change in expression of the unique miRNAs in BH exposure compared to sham.

from a pairing of each of the nine THz and BH-shared miRNAs [Fig. 11(b)]to all of the significantly differentially expressed mRNAs in THz or BH exposure. In this table, THz putative target mRNAs that were unique to THz or BH exposure as well as those that were shared in both exposures are highlighted. As shown, six of these miRNAs (miR-1827, miR-208a-3p,

miR-296-5p, miR-3617-5p, miR-517a-3p, and miR-576-5p) have one or few common target mRNAs. Of the remaining miRNAs, miR-362-5p and miR-526a have a totally different set of target mRNAs in THz radiation versus BH exposure whereas miRNA let-7a-5p has putative targets only in the THz radiation differentially expressed mRNAs.

TABLE I
COMPARISON OF THZ AND BH TARGET MRNAS FOR EACH SHARED MIRNA. EACH THZ RADIATION AND BH-SHARED MIRNAS WAS PAIRED WITH THE DISCOVERED DIFFERENTIALLY EXPRESSED MRNAS FROM THZ OR BH EXPOSURE USING IPA. (-) MEANS NO PUTATIVE TARGET MRNAS WERE FOUND

miRNA	THz Putative Target mRNAs	THz & BH Target mRNAs	BH Putative Target mRNAs
let-7a-5p	ACTA1, AGO4, BTN2A1, COL1A1, CPM, CYP19A1, DCLK3, DSP, DUSP16, DZIP1, EPHA3, FBXO32, FZD4, GABBR2, GHR, HAS2, HMGA2, ITGB3, LIMD1, LINGO1, MSR1, NOS1, OTUB2, PCYT1B, PLD5, PLXNA4, RHOB, SEMA4G, SFT2D3, SGCD, SLC4A7, SMUG1, SULF2, SYT11, TTLL4, WASL, ZBTB10, ZNF493	–	–
miR-1827	ADAMTS4, ARSB, ARSD, BLOC1S3, CACNB2, CALCA, CCDC68, CD300LF, CNN3, CORIN, COX6B2, CPM, CYP19A1, DEPDC1, ECE1, FAM53B, FCHO2, HOXC9, KHK, KLHL1, KY, LAMC2, LANCL2, LPCAT2, LRRC25, LRRC7, MAP3K15, MDH1B, NOS1, NPR3, PAPPA2, PLEKHA6, PLXNA4, PRRG1, PVRL4, PYCRL, RAPGEF5, SAMHD1, SIRT5, SLC10A1, SMIM10, SPATA18, SUSD5, SYT9, TAT, TNFRSF9, TRAK1	UBE3B	ADRA1A, AHNAK, APOL6, CACNA1G, CBFA2T2, CNFN, CYB561, DAND5, ESR1, FAM160B2, FAM217B, FAM46A, FGF18, FGFRL1, GAL3ST1, HEY1, IGF1, INPP5B, JAK3, JPH3, KIAA1755, MUL1, MUM1, NRG1, PIGV, PRKAA2, PSME4, RBPMS, RHO, SCML4, SERPINH1, SGPL1, SLC30A2, SMCR7, SMIM6, SOCS3, SPPL3, STRAP, TADA3, THBS1, THEM4, TMC5, TMED10, TMPRSS13, TRA2B, VIPR2, XG, ZBTB3, ZC3H12A, ZCCHC4, ZNF557, ZNF585B, ZNF689, ADAM30
miR-208a-3p	EPHA3, EPHA5, FZD4, SOS2, ARSD	BHLHE41	CD14, CELSR1, CNKSR2, COL4A3, EYA4, HIST2H2BE, MLF1, MTMR3, NAV2, PHLDA2, PURB, SRCIN1, YTHDC1, ZEB2
miR-296-5p	ABCF2, ACSL5, ADRA1D, AGFG2, ARHGEF4, ARSB, BLOC1S3, C9orf173, CD300LF, CNN1, COX18, ECE1, EHMT1, F9, FAM53B, FBXO31, FBXO32, FCRL5, FGF7, FGFR3, FZD4, GABBR2, GLI2, H1FX, IFNK, KHK, KIF1A, LINGO1, LITAF, LRCH4, MCAM, MRC2, NBEAL2, NCAM1, NOS1, OTUB2, PIEZO2, PYCRL, RAB11B, SIRT5, SLC1A7, SMOC2, SRRM3, SSTR1, SYDE2, SYT11, TC2N, TNFAIP2, TTLL4, VWA1, ZNF555	CD44 GPR173 HES5 MEOX1 NUMA1	APOL6, ATP2B3, AZU1, C11orf87, C19orf26, CAD, CADM3, CELSR1, CERS1, CHAC1, CMBL, DNAJB1, EPN3, FAM160B2, FAM169B, FAM19A5, FBN2, FCAMR, FGFBP2, FGFRL1, FMNL3, FZD10, GADD45G, GAL3ST1, GIGYF1, HELZ2, IL11, IL27, JPH3, KIAA2018, KLF10, KLHDC10, LRRC10B, LSMEM1, LTB4R, MAP3K8, MAP7D2, MEGF6, MMP11, NR2F6, NR4A3, PHOSPHO1, PNPLA7, POU3F1, RGS11, RHBDL3, SCAMP5, SNAI1, SPPL3, SRCIN1, ST3GAL3, TBC1D13, TECR, TLN1, TMEM132B, TMEM158, TPPP, USP22, VAC14, WDR20, XG, ZBTB42, ZNF585B, ACCS
miR-3617-5p	EPHA3, MFAP5, NPL, PGR, RAPGEF6, RNF17, SYDE2, TAC1, TRAK1, ZNF677, C1orf173	NPAS3 CD44	CDH8, EIF4A2, GLCCI1, HOXB2, HPCAL4, HTR2A, MS4A6A, NEFH, PRKAA2, SLC22A16, YTHDC1
miR-362-5p	C1orf173, C7, CYLD, DAZ2, DAZL, NPR3, OLIG3, RAPGEF6, RIPK2, SLITRK6, TRAK1, C18orf54	–	C15orf41, CLCA4, DLL1, DNAJB1, GPR98, MAP3K8, MLF1, MRC1, SLC35G3
miR-517a-3p	C1orf173, HPGDS, MYH4, RALGAPA1, SMIM10	BHLHE41	ANKRD29, CDKN1C, H2BFM, IGF1, IRF2BP2, LGALS13, MS4A4A, NPAS4, PDE4D, SIGLEC5, TNKS, WDR91
miR-526a	CASD1, CREBRF, CYLD, ELL2, FGF7, JPH4, MCF2L, MFAP5, MSR1, NPL, PRRG1, RALGAPA1, SFT2D3, SYDE2	–	ATF3, CCNL1, CDH8, CXCL11, DOCK5, EFNB2, MORC1, MRC1, SLC1A2, TNFRSF19, TNFSF10
miR-576-5p	CD36, FCHO2, HOPX	BHMT	C11orf87, DNAJB7, GJA5, ITPR1, KLF10, MGARP, NAMPT

Each THz radiation and BH-shared miRNAs was paired with the differentially expressed mRNAs from THz or BH exposure using IPA.
(-) means no putative target mRNAs were found.

IV. DISCUSSION AND CONCLUSION

In the present study, we aimed to perform a full transcriptional response of mRNAs and miRNAs and used these data to identify the intracellular canonical pathways that are triggered in THz-irradiated cells. We specifically sought to answer the following fundamental question: Do cells exposed to high-power 2.52 THz radiation exhibit similar or different specific cellular and molecular events compared to cells exposed to an equivalent dose (temperature rise and exposure time) conventional thermal BH?

In our experiments, a 40 min exposure of Jurkat cells to a CW, single-frequency, 2.52 THz produced about a 6 °C rise in temperature. Therefore, we included a matched 44 °C BH control for comparison. It is interesting to note that our results showed that cells exposed to 2.52 THz radiation differentially expressed a specific set of mRNAs and miRNAs than those differentially expressed in BH-exposed cells. In fact, less than 10% and 17% of the altered mRNAs and miRNAs, respectively, were shared by THz and BH exposures. As a result, we observed that these differentially expressed genes involve specific metabolic and

signaling pathways in THz radiation versus BH exposure when compared to the sham control.

It is known that a temperature increase due to heating can cause intracellular and membrane proteins to unfold, entangle, and aggregate [46]–[53]. Such modifications can preclude cells from functioning properly. Therefore, in order to overcome such stress and ensuing pleotropic effects, cells utilize their cellular defense and adaptation mechanism, commonly referred to as the cellular stress response (CSR). The CSR is rapidly activated in response to stressors such as heat, and a hallmark of this response is a change in expression of hundreds of genes [46]. The stress-inducible genes encode for a multitude of proteins involved in many important functions including: cellular survival, cell cycle control, and apoptosis; molecular chaperones, with the predominant class being heat shock proteins (Hsps); regulatory proteins, including transcription regulatory molecules, cytokines, and immediate early genes (IEGs); cell organization and structure, such as proteins required to sustain actin cytoskeleton; proteolysis (i.e., proteases); DNA sensing and repair; metabolism; and membrane regulation and transport [67], [68]. In this regard, it is not surprising that BH elicited a heat stress response in the exposed cells, which was manifested through a significant increase in the mRNAs encoding for molecular chaperoning proteins including the well characterized HSP70 (HSPA1A, HSPA6, HSPA1L and HSPA2) and HSP40 (DNAJB 1, 4 and 7), as well as smaller proteins like HSPB1 and HSPD1. Contrarily, although THz radiation induced a marked temperature rise (in the order of few degrees), it only caused an induction in HSPA1A and HSPA6. The expression of all the other mRNAs encoding for heat stress and chaperoning were not significantly changed by THz radiation, suggesting that, in our condition, 2.25-THz radiation does not appear to be directly damaging intracellular proteins.

Furthermore, BH exposure altered the expression of several other CSR gene functions such as proteolysis (MMP8, MMP11, MMP21, ADAM 12 and 30), extracellular matrix organization, cell growth, proliferation, or apoptosis (e.g., DUSPs JAK3, SGK1, GADD45B and 45G) in addition to transcription regulatory molecules and immediate early genes. THz radiation, on the contrary, had no significant effect on the expression of most of these genes. THz radiation exposure altered genes of the immune response (IL4 and IGHG1) and the expression of several genes involved in cell shape, adhesion, and cytoskeleton organization (e.g., ACTA1 and ACTA2, ITGB1, ITGB3 CDH19 and RHOB), which were not significantly changed in BH.

Our data, show that there is a discrepancy between the genes, metabolic and signaling pathways enriched for THz radiation versus BH exposure. They also provide evidence that THz radiation did not alter the expression of major heat shock chaperoning and proteolysis proteins that were affected in BH. Therefore, the results imply that 2.25-THz radiation does not appear to directly denature or significantly damage intracellular proteins and suggest that the heating regimen induced by THz radiation is different from that of the conventional thermal BH. Moreover, since the dynamics and vibrational motion of interfacial water differ considerably from that of bulk water, and, given that interfacial water absorption is maximal at ∼2.4–2.5 THz [12], we speculate that electromagnetic radiation at a frequency of 2.5 THz is preferentially coupled to and selectively absorbed by interfacial water molecules in living cells. This selective coupling mechanism might cause appreciable local temperature rises on the surface of biomolecules, triggering specific cellular responses not observed with the BH protocol. Nonetheless, using a different heating protocol than the conventional thermal BH, such as using a near IR beam, to generate a same temperature rise as THz, would be needed to validate our speculations.

Inherent gene regulation is fundamental to the versatility and adaptability of cells. Therefore, a change in such processes by an external stimulus such as THz radiation could lead to significant biochemical or physiological implications. Hence, the use of THz radiation as a non-contact tool for the selective targeting of specific gene programs would have a considerable impact in biotechnology and/or medicine. In such a scenario, THz radiation could potentially be used to selectively regulate key genes involved in specific pathways and cellular processes. Few examples include cellular reprogramming, cellular preconditioning, and nerve stimulation or repression [38], [39], [69], [70]. A recent study showed that exposure of mouse stem cells to 2.25-THz radiation caused gene specific transcriptional alterations and accelerated stem cell differentiation toward adipocytes [38], [39]. Furthermore, another study, showed the stimulating effect of THz radiation on nerve cells [70].

Our study provides valuable new insights that present a much clearer picture of intracellular canonical pathways that are specifically triggered in human cells exposed to high-power CW 2.52 THz. Further investigations involving other cell lines and primary cells with a variation in the THz exposure regimes, time courses, size, shape and doses of the THz beam and studies using a wide range of THz radiation frequencies are needed to validate our conclusions.

REFERENCES

[1] B. M. Ladanyi and M. S. Skaf, "Computer simulation of hydrogen-bonding liquids," *A. Rev. Phys. Chem.*, vol. 44, pp. 335–368, Oct. 1993.

[2] D. Russo, G. Hura, and T. Head-Gordon, "Hydration dynamics near a model protein surface," *Biophys J.*, vol. 86, no. 3, pp. 1852–1862, Mar. 2004.

[3] M. Hakala *et al.*, "Correlation of hydrogen bond lengths and angles in liquid water based on Compton scattering," *J. Chem. Phys.*, vol. 125, pp. 084504–084507, Oct. 2006.

[4] P. Wernet *et al.*, "The structure of the first coordination shell in liquid water," *Science*, vol. 304, no. 5673, pp. 995–999, May 2004.

[5] H. Yada *et al.*, "Origin of the fast relaxation component of water and heavy water revealed by terahertz time-domain attenuated total reflection spectroscopy," *Chem. Phys. Lett.*, vol. 464, no. 4–6, pp. 166–170, Oct. 2008.

[6] S. K. Pal, J. Peon, and A. H. Zewail, "Ultrafast surface hydration dynamics and expression of protein functionality: Alpha-Chymotrypsin," *Proc Nat. Acad. Scis USA*, vol. 99, pp. 15297–15302, Nov. 2002.

[7] S. K. Pal, J. Peon, and A. H. Zewail, "Biological water at the protein surface: Dynamical solvation probed directly with femtosecond resolution," *Proc Nat. Acad. Sci. USA*, vol. 99, pp. 1763–1768, Feb. 2002.

[8] S. K. Pal and A. H. Zewail, "Dynamics of water in biological recognition," *Chem. Rev.*, vol. 104, pp. 2099–212, Mar. 2004.

[9] S. K. Pal, L. Zhao, and A. H. Zewail, "Water at DNA surfaces: Ultrafast dynamics in minor groove recognition," *Proc. Nat. Acad. Sci. USA*, vol. 100, pp. 8113–8118, May 2003.

[10] M. S. Cheung, A. E. García, and J. N. Onuchic, "Protein folding mediated by solvation: Water expulsion and formation of the hydrophobic core occur after the structural collapse," *Proc. Nat. Acad. Sci. USA*, vol. 99, pp. 685–690, Jan. 2002.

[11] M. Chaplin, "Do we underestimate the importance of water in cell biology?," *Nat. Rev. Mol. Cell Biol.*, vol. 7, pp. 861–866, Nov. 2006.

[12] A. Orecchini *et al.*, "Water dynamics as affected by interaction with biomolecules and change of thermodynamic state: A neutron scattering study," *J. Phys. Condens. Matter.*, vol. 24, no. 6, p. 064105, Feb. 2012.

[13] U. Heugen *et al.*, "Solute-induced retardation of water dynamics probed directly by terahertz spectroscopy," *Proc. Nat.. Acad. Sci. USA*, vol. 103, no. 33, pp. 12301–12306, Aug. 2006.

[14] S. Ebbinghaus *et al.*, "An extended dynamical hydration shell around proteins.," *Proc. Nat. Acad. Sci. USA*, vol. 104, pp. 20749–20752, Dec. 2007.

[15] M. Walther *et al.*, "Far-infrared vibrational spectra of all-trans, 9-cis and 13-cis retinal measured by THz time-domain spectroscopy," *Chem. Phys. Lett.*, vol. 332, no. 3–4, pp. 389–395, Dec. 2000.

[16] T. Globus *et al.*, "THz-spectroscopy of biological molecules," *J. Biol. Phys.*, vol. 29, no. 2–3, pp. 89–100, Jun. 2003.

[17] A. Xie *et al.*, "Excited-state lifetimes of far-infrared collective modes in proteins," *J. Biol. Phys.*, vol. 28, no. 2, pp. 147–154, 2002.

[18] B. Fischer *et al.*, "Terahertz time-domain spectroscopy and imaging of artificial RNA," *Opt Exp.*, vol. 13, no. 14, pp. 5205–5215, Jul. 2005.

[19] B. M. Fischer, "Broadband THz time-domain spectroscopy of biomolecules," Ph.D. dissertation, Albert-Ludwigs-Universitat, Freiburg, Germany, 2005.

[20] K. J. Tielrooij *et al.*, "Dielectric relaxation dynamics of water in model membranes probed by terahertz spectroscopy," *Biophys. J.*, vol. 97, no. 9, pp. 2484–2492, Nov. 2009.

[21] T. Q. Luong *et al.*, "Do hydration dynamics follow the structural perturbation during thermal denaturation of a protein: A terahertz absorption study," *Biophys. J.*, vol. 101, no. 4, pp. 925–933, Aug. 2011.

[22] Y. He *et al.*, "Evidence of protein collective motions on the picosecond timescale," *Biophys. J.*, vol. 100, no. 4, pp. 1058–1065, Feb. 2011.

[23] G. P. Gallerano, "THz-Bridge: Tera-Hertz radiation in biological research, investigation on diagnostics and study of potential genotoxic effects (THz-Bridge)," [Online]. Available: http://www.frascati.enea.it/THz-BRIDGE/ Final Rep

[24] A. Ramundo-Orlando *et al.*, "Permeability changes induced by 130 GHz pulsed radiation on cationic liposomes loaded with carbonic anhydrase," *Bioelectromagn.*, vol. 28, no. 8, pp. 587–598, Dec. 2007.

[25] G. J. Wilmink *et al.*, "Determination of death thresholds and identification of terahertz (THz)-specific gene expression signature," in *Proc. SPIE 7562, Optical Interactions with Tissues and Cells XXI*, 2010, Paper 75620K.

[26] G. J. Wilmink and J. E. Grundt, "Invited review article: Current state of research on biological effects of terahertz radiation," *J. Infrared, Milli. TeraHz Waves*, vol. 32, no. 10, pp. 1074–1122, Oct. 2011.

[27] V. Pikov *et al.*, "Modulation of neuronal activity and plasma membrane properties with low-power millimeter waves in organotypic cortical slices," *J. Neural Eng.*, vol. 7, no. 4, Aug. 2010, Art. ID 045003.

[28] A. Ramundo-Orlando and G. P. Gallerano, "Terahertz radiation effects and biological applications," *J. Infrared, Milli. TeraHz Waves*, vol. 30, no. 12, pp. 1308–1318, Dec. 2009.

[29] A. Homenko *et al.*, "Effects of 100 GHz radiation on alkaline phosphatase activity and antigen-antibody interaction," *Bioelectromagn.*, vol. 30, no. 3, pp. 167–175, Apr. 2009.

[30] A. Korenstein-Ilan *et al.*, "Terahertz radiation increases genomic instability in human lymphocytes," *Radiat. Res.*, vol. 170, no. 2, pp. 224–234, Aug. 2008.

[31] G. J. Wilmink *et al.*, "In vitro investigation of the biological effects associated with human dermal fibroblasts exposed to 2.52 THz radiation," *Lasers Surg. Med.*, vol. 43, no. 2, pp. 152–163, Feb. 2011.

[32] L. V. Titova *et al.*, "Intense THz pulses down-regulate genes associated with skin cancer and psoriasis: A new therapeutic avenue?," *Scientific Reports*, vol. 3, p. 2363, Aug. 2013.

[33] L. V. Titova *et al.*, "Intense THz pulses cause H2AX phosphorylation and activate DNA damage response in human skin tissue," *Biomed. Opt. Exp.*, vol. 4, no. 4, pp. 559–568, Apr. 2013.

[34] G. J. Wilmink *et al.*, "Quantitative investigation of bioeffects associated with terahertz radiation," in *Proc. SPIE 7562, Optical Interactions With Tissues and Cells XXI*, 2010, Paper 75620L.

[35] J. E. Grundt *et al.*, "Terahertz radiation triggers a signature gene expression profile in human cells," in *Proc. IRMMW-THz*, 2011, pp. 1–2.

[36] G. J. Wilmink *et al.*, "Terahertz radiation preferentially activates the expression of genes responsible for the regulation of plasma membrane properties," in *Proc. IRMMW-THz*, 2011, pp. 1–3.

[37] B. S. Alexandrov *et al.*, "Non-thermal effects of terahertz radiation on gene expression in mouse stem cells," *Biomed. Opt. Exp.*, vol. 2, no. 9, pp. 2679–2689, Sep. 2011.

[38] J. Bock *et al.*, "Mammalian stem cells reprogramming in response to terahertz radiation," *PLoS One*, vol. 5, no. 12, p. e15806, Dec. 2010.

[39] B. S. Alexandrov *et al.*, "Specificity and heterogeneity of terahertz radiation effect on gene expression in mouse mesenchymal stem cells," *Sci. Rep.*, vol. 3, p. 1184, Jan. 2013.

[40] H. Frohlich, "The extraordinary dielectric properties of biological materials and the action of enzymes," *Proc. Nat. Acad. Sci. USA*, vol. 72, no. 11, pp. 4211–4215, Nov. 1975.

[41] S. M. Chitanvis, "Can low-power electromagnetic radiation disrupt hydrogen bonds in dsDNA?," *J. Polym. Sci. B, Polym. Phys.*, vol. 44, no. 18, pp. 2740–2747, Sep. 2006.

[42] B. S. Alexandrov *et al.*, "DNA breathing dynamics in the presence of a terahertz field," *Phys. Lett. A*, vol. 374, no. 10, pp. 1214–1217, 2010.

[43] B. S. Alexandrov *et al.*, "Toward a detailed description of the thermally induced dynamics of the core promoter," *PLOS Comput. Biol.*, vol. 5, no. 3, Mar. 2009, Art. ID e1000313.

[44] B. S. Alexandrov *et al.*, "DNA dynamics play a role as a basal transcription factor in the positioning and regulation of gene transcription initiation," *Nucleic Acids Res.*, vol. 38, no. 6, pp. 1790–1795, Apr. 2010.

[45] O. P. Cherkasova *et al.*, "Influence of terahertz laser radiation on the spectral characteristics and functional properties of albumin," *Opt. Spectrosc.*, vol. 107, no. 4, pp. 534–537, Oct. 2009.

[46] K. Richter *et al.*, "The heat shock response: Life on the verge of death," *Mol. Cell.*, vol. 40, no. 2, pp. 253–266, Oct. 2010.

[47] R. Schreck *et al.*, "Nuclear factor kappa B: An oxidative stress-responsive transcription factor of eukaryotic cells," *Free Radic. Res. Commun.*, vol. 17, no. 4, pp. 221–237, 1992.

[48] N. J. Millenbaugh *et al.*, "Gene expression changes in the skin of rats induced by prolonged 35 GHz millimeter-wave exposure," *Radiat. Res.*, vol. 169, no. 3, pp. 288–300, Mar. 2008.

[49] K. R. Diller, "Stress protein expression kinetics," *Annu. Rev. Biomed. Eng.*, vol. 8, pp. 403–424, 2006.

[50] D. Kultz, "Molecular and evolutionary basis of the cellular stress response," *Annu. Rev. Physiol.*, vol. 67, pp. 225–257, 2005.

[51] M. E. Feder and G. E. Hofmann, "Heat-shock proteins, molecular chaperones, the stress response: Evolutionary and ecological physiology," *Annu. Rev. Physiol.*, vol. 61, pp. 243–282, Mar. 1999.

[52] B. A. Miller, "The role of TRP channels in oxidative stress-induced cell death," *J. Membr. Biol.*, vol. 209, no. 1, pp. 31–41, Jan. 2006.

[53] A. E. Kabakov *et al.*, "Stressful preconditioning and HSP70 overexpression attenuate proteotoxicity of cellular ATP depletion," *Amer. J. Physiol. Cell Physiol.*, vol. 283, no. 2, pp. C521–534, Aug. 2002.

[54] V. Ambros, "microRNAs: Tiny regulators with great potential," *Cell*, vol. 107, no. 7, pp. 823–826, Dec. 2001.

[55] D. P. Bartel, "MicroRNAs: Genomics, biogenesis, mechanism, function," *Cell*, vol. 116, no. 2, pp. 281–297, Jan. 2004.

[56] L. P. Lim *et al.*, "The microRNAs of Caenorhabditis elegans," *Genes Dev.*, vol. 17, pp. 991–1008, Apr. 2003.

[57] B. P. Lewis *et al.*, "Conserved seed pairing, often flanked by adenosines, indicates that thousands of human genes are microRNA targets," *Cell*, vol. 120, no. 1, pp. 15–20, Jan. 2005.

[58] N. Rajewsky, "microRNA target predictions in animals," *Nat. Genet.*, vol. 38 Suppl, Jun. 2006, S8-13.

[59] Y. Benjamini *et al.*, "Controlling the false discovery rate in behavior genetics research," *Behav. Brain. Res.*, vol. 125, no. 1–2, pp. 279–284, Nov. 2001.

[60] S. Griffiths-Jones, "The microRNA Registry," *Nucl. Acids Res.*, vol. 32, pp. D109–111, Jan. 2004.

[61] S. Griffiths-Jones *et al.*, "miRBase: Microrna sequences, targets and gene nomenclature," *Nucl. Acids Res.*, vol. 34, pp. D140–144, Jan. 2006.

[62] I. Bentwich *et al.*, "Identification of hundreds of conserved and nonconserved human microRNAs," *Nat. Genet.*, vol. 37, no. 7, pp. 766–770, Jun. 2005.

[63] E. Berezikov *et al.*, "Phylogenetic shadowing and computational identification of human microRNA genes," *Cell*, vol. 120, no. 1, pp. 21–24, Jan. 2005.

[64] J. M. Cummins *et al.*, "The colorectal microRNAome," *Proc. Nat. Acad. Sci. USA*, vol. 103, no. 10, pp. 3687–3692, Feb. 2006.

[65] X. Xie *et al.*, "Systematic discovery of regulatory motifs in human promoters and 3' UTRs by comparison of several mammals," *Nature*, vol. 434, no. 7031, pp. 338–345, Feb. 2005.

[66] G. J. Wilmink *et al.*, "Identification of microRNAs associated with hyperthermia-induced cellular stress response," *Cell Stress Chap.*, vol. 15, no. 6, pp. 1027–1038, Nov. 2010.

[67] D. Kultz, "Evolution of the cellular stress proteome: From monophyletic origin to ubiquitous function," *J. Exp. Biol.*, vol. 206, no. 18, pp. 3119–3124, Sep. 2003.

[68] D. Kultz, "Molecular and evolutionary basis of the cellular stress response," *Annu. Rev. Physiol.*, vol. 67, pp. 225–257, 2005.

[69] G. J. Wilmink *et al.*, "Molecular imaging-assisted optimization of hsp70 expression during laser-induced thermal preconditioning for wound repair enhancement," *J. Invest. Dermatol.*, vol. 129, no. 1, pp. 205–216, Jan. 2009.

[70] M. V. Tsurkan *et al.*, "Changing growth of neurites of sensory ganglion by terahertz radiation," in *Proc. SPIE 8261, Terahertz Technology and Applications V*, 2012, Paper 82610S.

Ibtissam Echchgadda received the M.Sc. degree in medical and pharmaceutical research from the Free University of Brussels (VUB), Brussels, Belgium, in 1998, and the Ph.D. degree in cellular and structural biology and M.Sc. degree in clinical investigation from the University of Texas Health Science Center, San Antonio, San Antonio, TX. USA, in 2003 and 2010, respectively.

She currently is a Research Biological Scientist with the Air Force Research Laboratory (AFRL), 711 Human Performance Wing, Bioeffects Division, Radio Frequency Bioeffects Branch, Fort Sam Houston, TX, USA. Before joining AFRL, she was a Defense Contractor with General Dynamics Information Technology, served as a National Academy of Sciences Senior Associate, and before that was a Research Faculty Member with the University of Texas Health Science Center at San Antonio. Her current research focusses on investigating the biophysical and biochemical mechanisms that govern terahertz electromagnetic fields interaction with biological systems.

Jessica E. Grundt received the B.S. degree from the United States Air Force Academy, Colorado Springs, CO, USA, in 2008. She is currently working toward the M.D. degree. currently attends the School of Medicine at the University of Texas Health Science Center at San Antonio, TX, USA.

From 2009 to 2013, she was with the Air Force Research Laboratory, 711 Human Performance Wing, Bioeffects Division, Radio Frequency Bioeffects Branch, Fort Sam Houston, TX, USA, where she was involved with studies investigating terahertz radiation effects on biological systems.

Cesario Z. Cerna received the B.S. degree in general biology from Texas A & M University, Kingsville, TX, USA, in 1993.

He is currently a Scientist with General Dynamics Information Technology, JBSA Fort Sam Houston, TX, USA. He has worked with leading laboratories including, the Institute for Drug Development, National Oceanic and Atmospheric Administration. His current work investigates genomic, proteomic, and metabolic effects resulting from terahertz radiation exposures.

Caleb C. Roth was born in Bowie, TX, USA. He received the B.A. degree in biology from Austin College, Sherman, TX, USA, in 2000, and the M.Sc. degree in biology from the University of Texas at San Antonio, San Antonio, TX, USA, in 2003, both in biology. He is currently working toward the Ph.D. degree in radiation biophysics from University of Texas Health Science Center at San Antonio.

He is a SMART Scholar (The Science, Mathematics and Research for Transformation Scholarship for Service Program) cohort 2012. He studies the biological effects of nanosecond electrical pulse generated shock waves on cells grown in culture. He conducts research at the Air Force Research Laboratory, Radio Frequency Bioeffects Branch Laboratory, Fort Sam Houston, TX, USA.

Jason A. Payne received the B.S. degree in biomedical engineering and M.E. degree in electrical engineering from Texas A&M University, College Station, TX, USA, in 2001 and 2009, respectively.

He is currently a Research Biomedical Engineer with the Air Force Research Laboratory, 711 Human Performance Wing, Bioeffects Division, Radio Frequency Bioeffects Branch, Fort Sam Houston, TX, USA. His current research interests include modeling and simulation of RF-tissue interaction, particularly for high-power microwave, millimeter-wave, and terahertz energy.

Bennett L. Ibey received the Ph.D. degree in biomedical engineering from Texas A&M University, College Station, TX, USA, in 2006.

He is a Senior Research Biomedical Engineer in the Air Force Research Laboratory, 711 Human Performance Wing, Bioeffects Division, Radio Frequency Bioeffects Branch, Fort Sam Houston, TX, USA. His research interests have focused on the interaction between tissue and nanosecond pulsed electric fields and high-peak-power microwave bioeffects.

Gerald J. Wilmink received the B.S., M.Sc., and Ph.D. degrees in biomedical engineering from Vanderbilt University, Nashville, TN, USA, and the M.B.A. degree from the University of Texas at Austin, Austin, TX, USA.

He is the Founder and CEO of WiseWear, San Antonio, TX, USA. He served as a Research Biomedical Engineer with the Air Force Research Laboratory (AFRL), 711 Human Performance Wing, Bioeffects Division, Radio Frequency Bioeffects Branch, Fort Sam Houston, TX, USA. During his tenure at AFRL, he investigated the mechanisms that govern terahertz radiation interaction with biological systems.